Chemical Communications

COMMUNICATION

Enhancement of SOD activity in boehmite supported nanoreceptors

Received 00th January 20xx,
Accepted 00th January 20xx

DOI: 10.1039/x0xx00000x

www.rsc.org/

Álvaro Martínez-Camarena,[a] Estefanía Delgado-Pinar,[a] Concepción Soriano,[b] Javier Alarcón,[c] José M. Llinares,[a,b] Roberto Tejero[d] and Enrique García-España[a]

The binuclear Cu^{2+} complex of a pyridinophane polyamine ligand ranking amongst the fastest SOD mimetics so far reported displays a remarkable SOD activity enhancement when grafted to the surface of boehmite (γ-AlO(OH)) nanoparticles (BNPs).

The imbalance between the generation and clearance of reactive oxygen species (ROS) causes oxidative stress,[1] which is related to a variety of health issues that include cardiovascular diseases,[2] chronic inflammation,[3] diabetes,[4] neurodegenerative disorders such as Parkinson´s and Alzheimer Disease (AD),[5] cancer[6] and a variety of other age-related pathologies.[7] In order to remove ROS, living organisms have developed a battery of protective enzymes, such as superoxide dismutases (SODs), catalases and peroxidases. Mammalian SODs contain either CuZn-binuclear centres (SOD1 and SOD3) or Mn mononuclear centres (MnSOD, SOD2). Although SOD enzymes have shown therapeutic efficacy,[8] their use has severe drawbacks such as absence of oral activity, immunogenicity, short half-life and low cell permeability.[9] Therefore, low-molecular weight mimetics may offer better outcomes regarding properties such as lack of antigenicity, good tissue penetrance, high stability, longer half-life in solution, and low production cost.[10] A number of these low molecular SOD mimetics are complexes of polyamine ligands of either cyclic or open-chain topology.[11] In this respect, we have recently reported that several mononuclear or binuclear manganese and copper complexes[12] of aza-macrocyclic ligands[13] have SOD activities in vitro which rank among the highest ones so far reported for synthetic systems.[14]

A step forward to improve the activity, the likely-cell uptake and bio-distribution of these low molecular weight mimetics might be their incorporation in non-toxic nanoparticles (NPs). The grafting of the molecules to the surface of the nanoparticles may yield pre-concentration and amplification of the signal.[15]

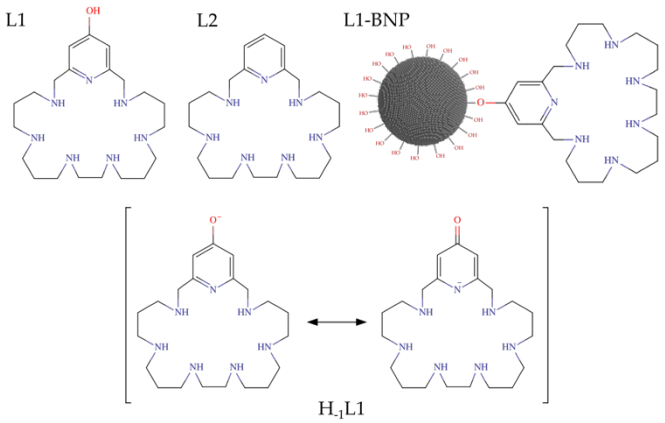

Fig. 1 Ligand drawing

As a proof of concept, here we report the synthesis of a new Cu^{2+} binucleating aza-macrocyclic ligand (L1) functionalized with a hydroxo group rightly disposed to permit its covalent anchorage to boehmite (γ-AlO(OH)) nanoparticles (BNPs) without loss of SOD activity. BNPs have been chosen as support because we and others[16] have shown its innocuous character that has permitted its use even as co-adjuvants in vaccines.[17] We discuss on the synthesis and coordinating ability of the free and grafted ligand as well as we provide information about the SOD activity of the different components involved in the nanoreceptor.

L1 was prepared using a modification of the Richman-Atkins procedure. 4-Benzyloxy-2,6-bis(bromomethyl)pyridine, prepared as described previously,[18] was reacted under reflux conditions with the pertosylated polyamine 1,5,9,13,17,21-hexakis(*p*-tolylsulfonyl)-1,5,9,13,17,21-hexaazaheneicosane[19] in dry CH_3CN using K_2CO_3 as a base. After purification of the tosylated macrocycle, by column chromatography, the tosyl groups were removed with a HBr/AcOH/PhOH mixture under reflux to obtain, after workup, L1·6HBr in good yield. Synthetic

[a] *ICMol, Departamento de Química Inorgánica, Universidad de Valencia, C/ Catedrático José Beltrán 2, 46980, Paterna, Spain.*
[b] *Departamento de Química Orgánica, Univesidad de Valencia, C/ Dr. Moliner s/n, 46100, Burjassot (Valencia), Spain.*
[c] *Departamento de Química Inorgánica, Universidad de Valencia, C/ Dr. Moliner s/n, 46100, Burjassot (Valencia), Spain.*
[d] *Departamento de Química Física, Universidad de Valencia, C/ Dr. Moliner s/n, 46100, Burjassot (Valencia), Spain.*
† Electronic Supplementary Information (ESI) available: See DOI: 10.1039/x0xx00000x

details and characterization data are included in the supplementary materials (Figure S1-S3). Afterwards, L1·6HBr was reacted with a suspension of BNPs in basic medium under reflux to graft the organic molecules onto the surface of the BNPs. Then, BNPs were exhaustively washed to obtain the final grafted material. The macrocyclic content of the material ($(0.35\pm0.04)\cdot10^{-4}$ mol/g_{BNP}) was deduced by elemental microanalysis and ^{1}H NMR spectroscopy (see Tables S1 and S2 and Figures S4 and S5 in the ESI). By ^{1}H NMR spectroscopy, a calibration using TMS as internal reference was made. The integration of the signals provided the amount of grafted organic molecules that were in agreement with those obtained from elemental microanalysis. Furthermore, the ICP-MS analysis was fully consistent with the previous data showing that there are two moles of complexed copper by every mole of grafted ligand (See ESI).

The BNPs were characterised by X-ray powder diffraction and dynamic light scattering (see Figures S6 and S7 in the ESI). The mean BNPs size was found to be about 58±30 nm. The X-ray powder diffraction pattern did not evidence any structural alteration due to the grafting process.

Previously to the studies with the grafted BNPs, we proceeded to characterise the Cu^{2+} complexation behaviour of L1 in solution. First, we measured by pH-metric titrations the protonation constants of L1, which are collected in Table S3. L1 shows seven protonation constants corresponding to the secondary amines and the phenol group which range between 10.68 and 4.14 logarithmic units. To know when the phenol group becomes protonated, we recorded UV spectra at variable pH. The variation of the band at 271 nm suggests that protonation of the phenol group occurs in the pH range 5-7 in correspondence with the formation of the H_5L1^{5+} species (Figure S8 in the ESI). As shown by the DFT studies, the wide pH range in which the non-protonated form prevails in solution might be related to the existence of a keto-enolic equilibrium. (Figure S9) Such equilibrium would be affording electron density to the pyridine nitrogen favouring hydrogen bonding interactions with neighbouring ammonium groups. Hence, L1 as it is illustrated in Fig. 1 does not really exist in solution at any pH since protonation of five of the amine groups would precede the protonation of the phenolate group.

pH-metric speciation studies at variable pH of the system Cu^{2+}-L1 show the formation of mononuclear species of $[CuH_xL]^{(2+x)}$ stoichiometry with x ranging from 4 to -1 and binuclear species of $[Cu_2L]^{4+}$ and $[Cu_2(H_{-1}L)]^{3+}$ stoichiometries (Figure 2). Mono- and binuclear hydroxylated species of $[Cu(H_{-1}L)(OH)]$, $[Cu_2(H_{-1}L)(OH)]^{2+}$ and $[Cu_2(H_{-1}L)(OH)_2]^{+}$ stoichiometries were also detected. The distribution diagram collected in Figs. 2 and S10 show that while for mole ratio Cu^{2+}:L1 1:1 only the mononuclear species are found in solution, for a 2:1 ratio the binuclear species prevail above pH 3. Interestingly, the UV spectra show that deprotonation of the phenolic group occurs as soon as the first Cu^{2+} binds to the macrocycle suggesting that the pyridine nitrogen is always involved in the coordination. The large values of the stability constants found for the complexes $[Cu(H_{-1}L)]^{+}$ and $[CuH(H_{-1}L)]^{2+}$ (entries 6 and 11 in Table S4) suggest that Cu^{2+} is coordinated,

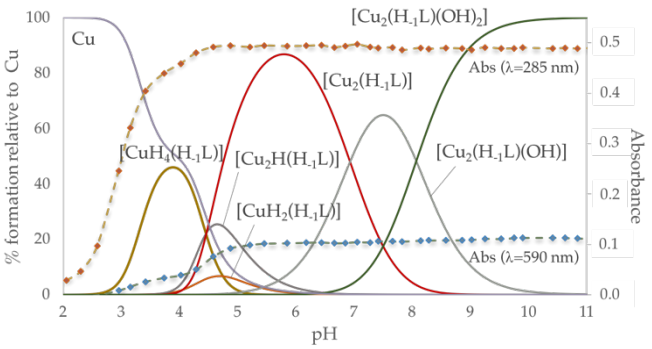

Fig. 2 Distribution diagram of the Cu^{2+}:L1 system as a function of the pH in aqueous solution. The UV-vis spectroscopic parameters at 285 nm (red dots) and at 590 nm (blue dots) are overlaid.

apart from the pyridine nitrogen atom, by other four amine groups of the macrocyclic cavity as it is also supported by the DFT calculations (see Figure 3A and Tables S5 and S6). So, the addition of a second Cu^{2+} is accompanied by much lower stability constants (entries 8 and 13 in Table S4) that can be ascribed to a lower number of nitrogen atoms participating in its coordination. Moreover, some bond breaking and reorganisation might accompany this second step. At this stage, the first metal ion might be coordinated by the pyridine nitrogen and three neighbouring polyamine nitrogen atoms, whereas the second Cu^{2+} would be bound to the remaining three amine groups. The second metal ion would complete its coordination sphere with two water molecules coming from the media. At higher pH, formation of two binuclear hydroxo species occurs being the pKa for the deprotonation of the water molecules, particularly the first one pKa = 7.26, rather low suggesting that the hydroxide ion behaves as a bridging ligand between both metal centres as supported also by the DFT calculations (see Figure 3B and Tables S7 and S8).

The unsaturated coordination sphere of the second metal ion and consequent reduced stability of the Cu^{2+} complex at this stage should lead to a better cycling between oxidation states Cu(II) and Cu(I) required for an efficient SOD activity to occur (Table S11 and Figure S11).

Since mammalian SOD1 and SOD3 contain Cu and Zn in their active centres, we have also investigated the coordination of Zn^{2+} and the formation of mixed Cu^{2+}-Zn^{2+} complexes by L1. The analysis of the pH-metric titrations shows similar speciation for Zn^{2+} and for Cu^{2+} (Table S9). However, the highest protonated mononuclear species detected is, in this case, $[Zn(H_3L)]^{5+}$ and only binuclear hydroxo-species are observed ($[Zn_2(H_{-1}L)(OH)]^{2+}$, $[Zn_2(H_{-1}L)(OH)_2]^{+}$ and $[Zn_2(H_{-1}L)(OH)_3]$). As expected, the

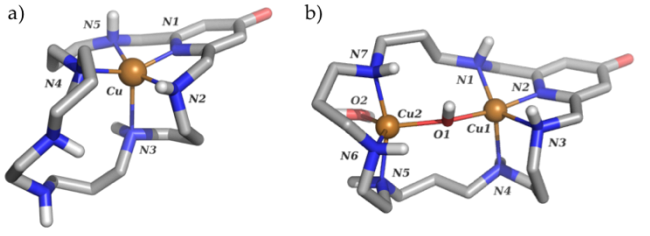

Fig. 3 DFT optimized structure of Cu^{2+}:L1 complex at physiological pH (7.40) a) Cu^{2+}:L1 1:1, b) Cu^{2+}:L1 1:2, b).

stability of the Zn^{2+} complexes is markedly lower than that of the Cu^{2+} ones. The pH range in which the $[Zn_2(H_{-1}L)(OH)]^{2+}$ hydroxylated species exist in solution suggests again a bridging binding mode for the hydroxide ligand. The variation of the UV spectra of the Zn^{2+}-L1 system indicates that, as happened for Cu^{2+}, deprotonation of the phenolic group also occurs as soon as the complexes start to form (Figure S12).

To obtain the constants for the mixed Cu^{2+}-Zn^{2+}-complexes we carried out potentiometric titrations of solutions containing Cu^{2+}, Zn^{2+} and L1 in a 1:1:1 molar ratio. In a first run of the fitting, we kept constant the values of the stability constants of the binary Cu^{2+}-L1, and Zn^{2+}-L1 complexes, previously obtained, and we proceed to determine only the values of the constants of the mixed Cu^{2+}-Zn^{2+} complexes (Table S10). To check the reliability of our data, in the final run of the fitting we treated simultaneously the titrations of the binary and tertiary systems leaving free all the stability constants for the Cu^{2+}-L1, Zn^{2+}-L1 and Cu^{2+}-Zn^{2+}-L1 systems obtaining values which agreed within the experimental errors with the previous ones. The mixed complexes had $[CuZn(H_{-1}L)]^{3+x}$ and $[CuZn(H_{-1}L)(OH)_n]^{(3-n)}$ stoichiometries with n = 1,2. As shown in the distribution diagram in Fig. S13 these mixed species predominate in solution only above pH 7.5. Again, the variation of the UV spectra with pH suggest that in all mixed complexes the phenol group is deprotonated either in the phenolate or the keto forms.

Once the Cu^{2+} and Zn^{2+} coordination chemistry in solution had been characterised, we proceeded to perform SOD activity assays by using the nitroblue tetrazolium (NBT) method.[20] The values of IC_{50} (defined as the amount of compound necessary for achieving 50% inhibition of NBT reduction -to blue formazan by the superoxide anion) and k_{cat} are collected in Table 1. Blank experiments were performed with the free ligands without observing any significant activity. Data of the binuclear complex of L2, the ligand without the phenol group,[19] are also included in Table 1 by means of comparison. First, it has to be pointed out that, as shown in the bar diagram of Fig. 4, the IC_{50} and k_{cat} values obtained for the two non-supported complexes rank amongst the most active ones so far reported in the literature.[8b,9,21] Second, the activity of the binuclear complex is much higher than those of the mononuclear complex of L1 and of the Cu^{2+}-Zn^{2+} mixed complex. As above commented, the Cu^{2+} coordination sphere in the mononuclear complex will be saturated by the pyridine and amine donors leading to a highly stable Cu^{2+} complex being, therefore, the reduction to Cu^{+} thermodynamically unfavourable. The unsaturated coordination sphere of the second Cu^{2+} and lower stability of this centre would make easier the cycling between oxidation states II and I necessary for the ping-pong mechanism of SOD to occur.

Finally, the anchoring of the macrocyclic binuclear complex to the BNPs leads to a very significant 8-fold increase in SOD activity. This amplification of activity may be related, as previously described for other systems,[15] to the pre-concentration of Cu^{2+} complexes in the surface of the BNPs that would favour their interaction with the substrate.

Table 1 SOD activity for the studied systems obtained by McCord-Fridovich test.

System	IC_{50} (μM)	k_{cat} (10^6 $M^{-1}s^{-1}$)
Cu_2L1	**0.8(1)**	**4.08**
$CuL1$	**1.4(5)**	**2.50**
$CuZnL1$	**1.6(2)**	**2.11**
Cu_2L1-BNPs	**0.10(3)**	**33.72**
Cu_2L2	**1.2(2)[b]**	**2.37[b]**
Cu_2Zn_2SOD	**0.010(2)[b]**	**430[b]**

[e] *Values in parentheses are standard deviations in the last significant figure. Measurements were performed in triplicate.*
[f] *Values obtained from bibliography.*[19,22]

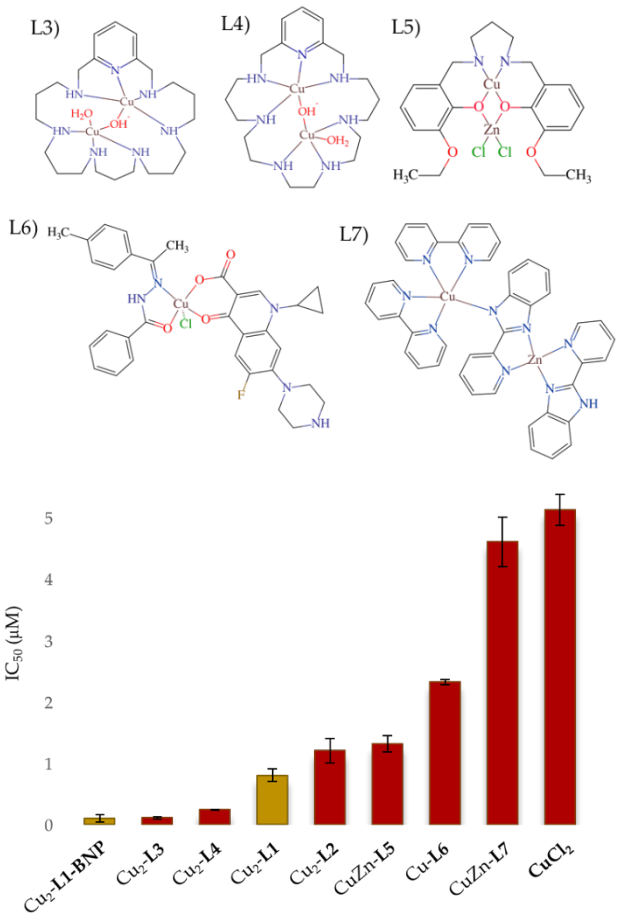

Fig. 4 Antioxidant activity of the systems Cu_2L1 and Cu_2L1-BNP and comparison with the activity of different Cu^{2+} complexes from bibliography: L3,[19] L4,[19] L5,[23] L6,[24] and L7.[25]

In spite that there is still a lot of work to be done in finding better and more diverse ways of anchorage of the macrocycles that permit more robust bonds to be formed and the grafting to NPs of different nature, the results here presented constitute a proof concept of a plausible way of getting improved efficiencies in SOD activity. On the other hand, these results also open a way to cover other important issues in drug

delivery and taxying; the inclusion of directing groups or related functions may contribute to this purpose. Currently, we are focusing our research efforts in these aspects.

Conflicts of interest

There are no conflicts to declare.

Acknowledgements

Financial support by the Spanish Ministerio de Economía y Competitividad (Projects CTQ2013-48917-C3-1-P, CTQ2016-78499-C6-1-R and Unidad de Excelencia MDM 2015- 0038) and Generalitat Valenciana (Project PROMETEOII2015-002) is gratefully acknowledged. One of us A. M-C. wants to thank Spanish Ministry of Education, Culture and Sport for the PhD grant FPU14/05098.

Notes and references

1 B. Haliweel and J. M. C. Gutteridgen, *Free Radicals in Biology and Medicine*, Claredon Press, 1989.
2 U. Singh and I. Jialal, *Pathophysiology*, 2006, **13**, 129-142.
3 D. Salvemini, T. M. Doyle and S. Cuzzocrea, *Biochem. Soc. Trans.*, 2006, **34**, 965-970.
4 A. C. Maritim, R. A. Sanders and J. B. Watkins III, *Biochem. Mol. Toxicol.*, 2003, **17**, 24-38.
5 *(a)* P. A. Kocatürk, M. C. Akbostanci, F. Tan and G. O. Kavas, *Pathophysiology*, 2000, **7**, 63-67; *(b)* Y. Ihara, M. Chuda, S. Kuroda and T. Hayabara, *J. Neurol. Sci.*, 1999, **170**, 90-95; *(c)* M. De Leo, S. Borrello, M. Passatino, B. Palazzotti, A. Mordente, A. Daniele, V. Filippini, T. Galeotti and C. Masullo, *Neurosci. Lett.*, 1998, **250**, 173-176; *(d)* V. Chauhan and A. Chauhan, *Pathophysiology*, 2006, **13**, 195-208.
6 *(a)* C. J. Weydert, T. A. Waugh, J. M. Ritchie, K. S. Iyer, J. L. Smith, L. Li, D. R. Spitz and L. W. Oberley, *Free Radic. Biol. Med.*, 2006, **41**, 226-237; *(b)* Y. Toh, S. Kuninaka, M. Mori, T. Oshiro, Y. Ikeda, H. Nakashima, H. Baba, S. Kohnoe, T. Okamura and K. Sugimachi, *Oncology*, 2000, **59**, 223-228; *(c)* R. H. Burdon, *Free Radic. Biol. Med.*, 1995, **18**, 775-794.
7 J. A. Vinson, *Pathophysiology*, 2006, **13**, 151-162.
8 *(a)* I. Batinić-Haberle, J. S. Rebouças and I. Spasojević, *Antioxid. Redox. Signal.*, 2010, **13**, 877-918; *(b)* C. Muscoli, S. Cuzzocrea, D. P. Riley, J. L. Zweier, C. Thiemermann, Z.-Q. Wang and D. Salvemini, *Br. J. Pharmacol.*, 2003, **140**, 445-460.
9 D. P. Riley, *Chem. Rev.*, 1999, **99**, 2573-2587.
10 (a) S. Cuzzocrea, E. Mazzon, R. Di Paola, T. Genovese, C. Muià, A. P. Caputi, D. Salvemini and A. Dunton, *Arthritis Rheum.*, 2005, **52**, 1929-1940; *(b)* W. Munroe, C. Kingsley, A. Durazo, E. Butler Gralla, J. A. Imlay, C. Srinivasan and J. Selverstone Valentine, *J. Inorg. Biochem*., 2007, **101**, 1875–1882; *(c)* W. B. Motherwell, M. J. Bingham and Y. Six, *Tetrahedron*, 2001, **57**, 4663–4686; *(d)* A. J. Kirby, *Angew. Chemie Int. Ed. English*, 1996, **35**, 706–724.
11 *(a)* K. Aston, N. Rath, A. Naik, U. Slomczynska, O. F. Schall and D. P. Riley, *Inorg. Chem.*, 2001, **40**, 1779–1789; *(b)* G.-F. Liu, M. Filipović, F. W. Heinemann and I. Ivanović-Burmazović, *Inorg. Chem.*, 2007, **46**, 8825–8835; *(c)* A. Dees, A. Zahl, R. Puchta, N. J. R. Van Eikema Hommes, F. W. Heinemann and I. Ivanović-Burmazović, *Inorg. Chem.*, 2007, **46**, 2459–2470; *(d)* M. Tamura, Y. Urano, K. Kikuchi, T. Higuchi, M. Hirobe and T. Nagano, *J. Organomet. Chem.*, 2000, **611**, 586–592; *(e)* D. Zhang, D. H. Busch, P. L. Lennon, R. H. Weiss, W. L. Neumann and D. P. Riley, *Inorg. Chem.*, 1998, **37**, 956–963.
12 V. Amendola, L. Fabbrizzi, C. Mangano and P. Pallavicini, *Acc. Chem. Res.*, 2001, **34**, 488–493.
13 J. González, J. M. Llinares, R. Belda, J. Pitarch, C. Soriano, R. Tejero, B. Verdejo and E. García-España, *Org. Biomol. Chem.*, 2010, **8**, 2367–2376.
14 *(a)* M. P. Clares, S. Blasco, M. Inclán, L. del C. Agudo, B. Verdejo, C. Soriano, A. Doménech, J. Latorre and E. García-España, *Chem. Commun.*, 2011, **47**, 5988–5990; (b) J. González-García, À. Martínez-Camarena, B. Verdejo, M. P. Clares, C. Soriano, E. García-España, H. R. Jiménez, A. Doménech-Carbó, R. Tejero, E. Calvo, L. Briansó-Llort, C. Serena, S. Trefler and A. Garcia-España, *J. Inorg. Biochem.*, 2016, **163**, 230–239.
15 C. Fasting, C. A. Schalley, M. Weber, O. Seitz, S. Hecht, B. Koksch, J. Dernedde, C. Graf, E. W. Knapp and R. Haag, *Angew. Chemie Int. Ed.*, 2012, **51**, 10472–10498.
16 A. Rutenberg, V. V. Vinogradov and D. Avnir, *Chem. Commun.*, 2013, **49**, 5636–5638.
17 B. Sun and T. Xia, *J. Mater. Chem. B*, 2016, **4**, 5496–5509.
18 *(a)* P. Froidevaux, J. M. Harrowfield and A. N. Sobolev, *Inorg. Chem.*, 2000, **39**, 4678–4687; *(b)* E. Busto, A. González-Álvarez, V. Gotor-Fernández, I. Alfonso and V. Gotor, *Tetrahedron*, 2010, **66**, 6070–6077.
19 R. Belda, S. Blasco, B. Verdejo, H. R. Jiménez, A. Doménech-Carbó, C. Soriano, J. Latorre, C. Terencio and E. García-España, *Dalton Trans.*, 2013, **42**, 11194–11204.
20 M. M. Tarpey and I. Fridovich, *Circ. Res.*, 2001, **89**, 224–237.
21 A. Nebot-Guinot, A. Liberato, M. A. Máñez, M. P. Clares, A. Doménech, J. Pitarch-Jarque, A. Martínez-Camarena, M. G. Basallote and E. García-España, Inorganica Chim. Acta, 2018, **472**, 139-148.
22 H. Ohtsu, Y. Shimazaki, A. Odani, O. Yamauchi, W. Mori, S. Itoh and S. Fukuzumi, *J. Am. Chem. Soc.*, 2000, **122**, 5733–5741.
23 C. Wang, S. Li, D. J. Shang, X. L. Wang, Z. L. You and H. B. Li, *Bioorganic Med. Chem. Lett.*, 2011, **21**, 4320–4324.
24 M. N. Patel, C. R. Patel and H. N. Joshi, *Appl. Biochem. Biotechnol.*, 2013, **169**, 1329–1345.
25 Y.-C. Fang, Y.-P. Chen, C.-T. Chen, T.-S. Lin and C.-Y. Mou, *J. Mater. Chem. B*, 2013, **1**, 6042-6052.

